Metallophysics and Advanced Technologies
Металофіз. новітні технол.
Metallofiz. Noveishie Tekhnol.
2026, vol. 48, No. 9, pp. 999–1010
https://doi.org/10.15407/mfint.48.09.0999
Reprints available directly from the publisher

© 2026 G. V. Kurdyumov Institute for Metal Physics,
National Academy of Sciences of Ukraine
Published by license under
the G. V. Kurdyumov Institute for Metal Physics–
N.A.S. of Ukraine Publishers imprint.
Printed in Ukraine.

PACS numbers: 07.05.Fb, 61.66.Fn, 68.37.Hk, 68.55.Nq, 72.20.Pa, 72.40.+w, 81.15.Cd

Fabrication and Characterization of CuO/Cu_2O Thin-Film Heterostructures on Si/ZnO Substrates *via* Magnetron Sputtering for Photovoltaic Applications

I. O. Kosimov[*], Sh. T. Khozhiev[*,**], K. T. Dovranov[***],
M. A. Davlatov[****], F. F. Arzikulov[**,******], U. Kh. Kholiqov[*****]

[*]*O. S. Sodikov Institute of Bioorganic Chemistry,*
Academy of Sciences of the Uzbekistan Republic,
83 Mirzo Ulugbek Ave.,
UZ-100125 Tashkent, Republic of Uzbekistan
[**]*Tashkent State Medical University,*
2 Farabi Str.,
UZ-100109 Tashkent, Republic of Uzbekistan
[***]*Karshi State University,*
17 Kuchabag Str.,
UZ-180119 Karshi, Republic of Uzbekistan
[****]*Karshi State Technical University,*
225 Mustaqillik Ave.,
UZ-180100 Karshi, Republic of Uzbekistan
[*****]*Termez State University of Engineering and Agricultural Technologies,*
228A Islom Karimov Str.,
UZ-190100 Termez, Republic of Uzbekistan

In this work, CuO and Cu_2O thin-film heterostructures are fabricated on Si/ZnO substrates using the magnetron sputtering technique under varying substrate preparation conditions. The deposition process is performed in three modes: without substrate heating, with heating at 600°C, and with

Corresponding author: Isroil Odinaevich Kosimov
E-mail: isroilkosimov@list.ru

Citation: I. O. Kosimov, Sh. T. Khozhiev, K. T. Dovranov, M. A. Davlatov, F. F. Arzikulov, and U. Kh. Kholiqov, Fabrication and Characterization of CuO/Cu_2O Thin-Film Heterostructures on Si/ZnO Substrates *via* Magnetron Sputtering for Photovoltaic Applications, *Metallofiz. Noveishie Tekhnol.*, **48**, No. 9: 999–1010 (2026), DOI: 10.15407/mfint.48.09.0999

© Publisher PH 'Akademperiodyka' of the NAS of Ukraine, 2026. This is an open access article under the CC BY-ND license (https://creativecommons.org/licenses/by-nd/4.0)

heating at 600–800°C followed by glow discharge ion cleaning. Comprehensive characterization is carried out to investigate the crystallinity, phase composition, surface morphology, and optical properties of the films. X-ray diffraction (XRD) analysis reveals that high-temperature heating combined with ion cleaning results in well-crystallized, dense, and smooth films with a pure-phase composition. Particularly, Cu_2O films grown on ion-cleaned substrates at 800°C exhibited 100% crystalline-phase formation. Scanning electron microscopy (SEM) and energy-dispersive spectroscopy (EDS) confirmed the uniform distribution of nanosize grains, while Raman spectroscopy validated the phase identification of CuO and Cu_2O. The results indicate that optimizing substrate temperature and surface pretreatment significantly enhances the structural and optical quality of copper-oxide semiconductor layers. The fabricated CuO/Cu_2O heterostructures demonstrate strong potential for use in efficient and environmentally friendly solar-cell devices.

Key words: CuO, Cu_2O, thin films, magnetron sputtering, heterostructures, crystallinity, SEM, Raman spectroscopy, solar cells.

У цій роботі тонкоплівкові гетероструктури CuO і Cu_2O були виготовлені на підкладинках Si/ZnO за допомогою методи магнетронного напорошення за різних умов підготовки підкладинки. Процес осадження проводився у трьох режимах: без нагрівання підкладинки, з нагріванням до 600°C та з нагріванням до 600–800°C із подальшим очищенням йонами жеврійного розряду. Було проведено всебічну характеризацію для дослідження кристалічности, фазового складу, морфології поверхні й оптичних властивостей плівок. Рентґенівська дифракційна аналіза (XRD) показала, що високотемпературний нагрів у поєднанні з йонним очищенням приводить до формування добре кристалізованих, щільних і гладких плівок із чистим фазовим складом. Зокрема, плівки Cu_2O, вирощені на очищених йонами підкладинках за 800°C, продемонстрували формування 100% кристалічної фази. Сканувальна електронна мікроскопія (CEM) та енергодисперсійна спектроскопія (EDS) підтвердили рівномірний розподіл нанорозмірних зерен, а Раманова спектроскопія верифікувала фазову ідентифікацію CuO та Cu_2O. Результати свідчать, що оптимізація температури підкладинки та попереднє оброблення поверхні істотно підвищує структурну й оптичну якість напівпровідникових шарів оксиду Купруму. Створені гетероструктури CuO/Cu_2O демонструють високий потенціял для використання у високоефективних та екологічно чистих сонячних елементах.

Ключові слова: CuO, Cu_2O, тонкі плівки, магнетронне розпорошення, гетероструктури, кристалічність, CEM, Раманова спектроскопія, сонячні елементи.

(Received 16 August, 2025; in final version, 16 June, 2026)

1. INTRODUCTION

In the modern era, the generation, storage, and efficient transmission of energy remain among the most critical global challenges. Research

efforts in this domain are largely focused on the development of cost-effective and high-performance materials for energy producing, storing, and delivery systems.

Over the past several decades, copper (Cu) has been extensively employed in semiconductor technology as a contact metal. Replacing aluminium, which was previously dominant, copper has become an essential component in high-temperature-resistant semiconductor devices. Notably, copper atoms possess a significantly higher diffusion coefficient in materials such as silicon and germanium [1].

Copper (I) oxide (CuO) has emerged as a promising candidate for solar cell applications. This is attributed to its high optical absorption coefficient, excellent chemical and thermal stability, nontoxic nature, lower production cost compared to materials like Ni, Ag, and Au, natural abundance, and outstanding optical, electrical, magnetic, and catalytic properties [2–5].

Although magnetron sputtering has previously been used to fabricate CuO and Cu_2O thin films [6–8], the present work reports, for the first time, the growth of such films on Si substrates preheated to 600°C and subjected to glow discharge ion cleaning prior to deposition. Copper oxide thin films can be synthesized using various techniques, including sol–gel, pulsed laser deposition, pyrolysis, chemical vapour deposition, and magnetron sputtering (the latter being particularly advantageous for achieving uniform surface morphology) [11–18].

In this study, CuO/ZnO/Si and Cu_2O/ZnO/Si heterostructures were fabricated *via* magnetron sputtering, with the ZnO/Si substrates preheated to 600°C and cleaned by glow-discharge ion bombardment. The effects of thermal treatment and gamma irradiation on the structural and morphological characteristics of the heterostructures were examined using x-ray diffraction phase analysis, scanning electron microscopy, and complementary characterization techniques.

2. EXPERIMENTAL/THEORETICAL DETAILS

The effect of thermal treatment on the electronic properties of Cu_2O/ZnO heterostructures grown by the magnetron sputtering method was investigated. In the heterojunction, ZnO was employed as a *p*-type and Cu_2O as an *n*-type semiconductor. To achieve surface uniformity and smoothness, an optimal regime was developed for heating the Si substrate to 600°C followed by cleaning under glow-discharge ion bombardment. The samples were deposited using a direct-current magnetron sputtering system, with a copper (Cu) target in an $Ar–O_2$ inert gas mixture (Fig. 1).

In this study, CuO and Cu_2O thin films were deposited onto Si/ZnO substrates under three different experimental conditions in an $Ar–O_2$ inert gas atmosphere using a Cu target:

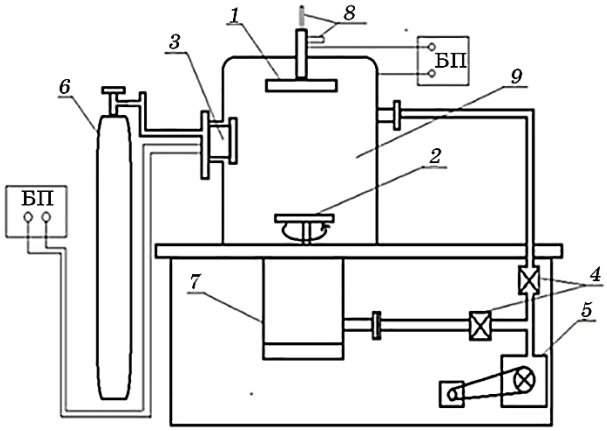


Fig. 1. Schematic diagram of the magnetron sputtering system: *1*—magnetron, *2*—target, *3*—ionizer, *4*—solenoid valve, *5*—fore pump, *6*—gas cylinder, *7*—diffusion pump, *8*—cooling system, *9*—vacuum chamber.

Condition 1—direct deposition without any pre-treatment of the substrate;
Condition 2—deposition after heating the substrate to 600°C;
Condition 3—deposition after heating the substrate to 600°C and performing glow discharge ion cleaning.

The crystallographic structure of the thin films prepared under these three conditions was examined using x-ray diffraction (Rigaku), while the degree of crystallinity and crystallite size were determined by x-ray phase analysis. Surface morphology, layer formation, and emission characteristics were studied using scanning electron microscopy (SEM). Structural changes and material characteristics were further analysed *via* Raman spectroscopy [19]. In addition, the electrical and optical properties of the films were systematically evaluated.

3. RESULTS AND DISCUSSION

In this study, a single-layer epitaxial structure KDP 0.5–1bk 2(III) standard silicon substrate was used. The x-ray phase analysis of this substrate is shown in Fig. 2, where characteristic diffraction peaks corresponding to silicon were observed at diffraction angles $2\theta \cong 28.5°$, 48.2°, 57.3°, 69.8°, and 76.7°, with interplanar spacings $d_{hkl} \cong 3.13$ Å, 1.91 Å, 1.63 Å, 1.35 Å, and 1.24 Å, respectively, corresponding to Miller indices (*hkl*) of (111), (202), (311), (400), and (313).

From these results, it can be concluded that the absence of additional phase peaks confirms the high purity of the silicon substrate. Initially, the Si substrate was heated to 300°C, and under identical deposition

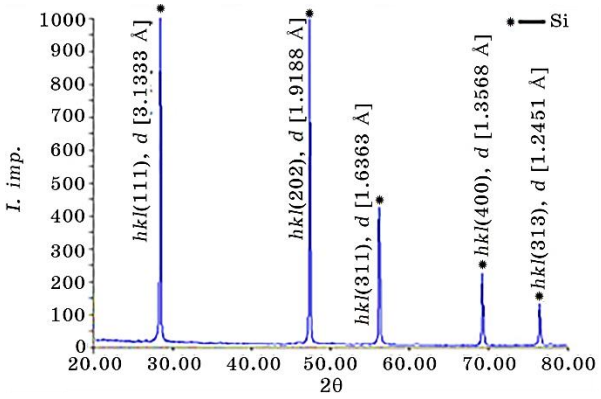


Fig. 2. X-ray phase analysis of the Si substrate sample.

conditions, three identical thin ZnO layers were grown on its surface using the magnetron sputtering method. The x-ray phase analysis of the ZnO-coated sample is shown in Fig. 3, while the SEM images are presented in Fig. 4 (*a*–*c*), and the EDS analysis in Fig. 5.

The x-ray phase analysis in Fig. 3 shows that in the Si/ZnO sample, the diffraction peaks of the Si phase were observed at $2\theta \cong 28.5°$ and 69.2°, corresponding to interplanar spacings $d_{hkl} \cong 3.13$ Å and 1.36 Å, with Miller indices (111) and (400), respectively. The ZnO phase exhibited diffraction peaks at $2\theta \cong 31.8°$, 34.4°, 36.3°, 47.5°, 56.6°, 62.8°, 66.4°, 68.0°, 69.1°, and 77.0°, corresponding to $d_{hkl} \cong 2.81$ Å, 2.60 Å, 2.47 Å, 1.91 Å, 1.24 Å, 1.48 Å, 1.41 Å, 1.38 Å, 1.24 Å, and Miller indices (100), (002), (101), (012), (110), (013), (200), (112), and (202), re-

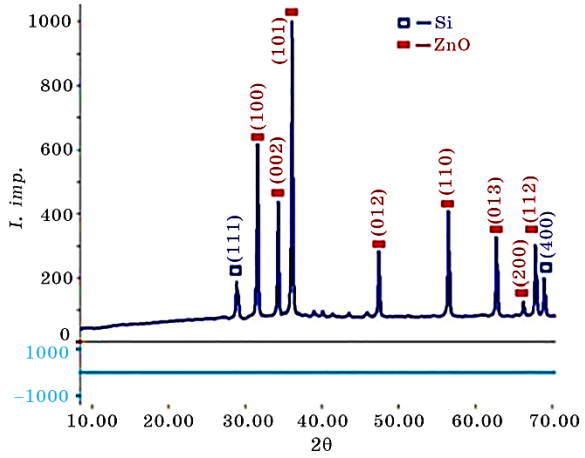


Fig. 3. X-ray phase analysis of the ZnO thin film grown on the Si substrate under identical deposition conditions by magnetron sputtering.

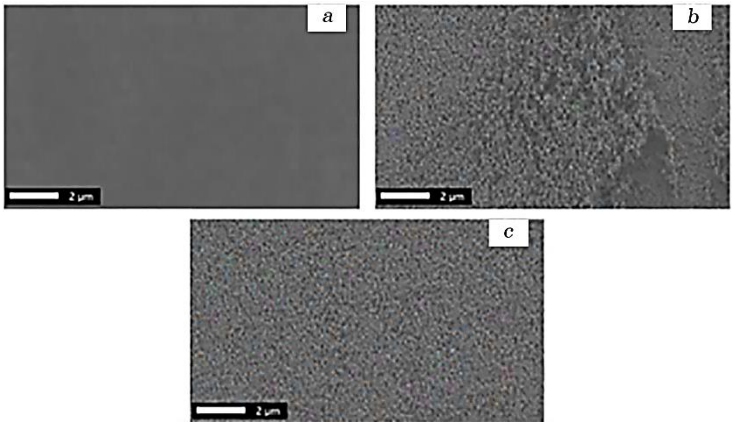


Fig. 4. SEM micrographs: *a*—Si substrate; *b*—Si/ZnO grown at 300°C; *c*—Si/ZnO grown at 600°C.

spectively.

Figure 4 (*a*–*c*) presents the SEM images of Si/ZnO samples grown under three different conditions: without heating, heated to 300°C, and heated to 600°C prior to ZnO deposition. In Figure 4*a*, corresponding to the unheated Si substrate with a ZnO thin film, the surface appears smooth and uniformly arranged. In Figure 4*b*, representing the sample grown at 300°C, the SEM image shows that ZnO nanoparticles are irregularly shaped and unevenly distributed over the surface. In contrast, Fig. 4*c*, corresponding to growth at 600°C, reveals a well-ordered surface morphology with good adhesion, where dense, spherical structures are formed. The surface is fully covered with uniformly distributed, pure-phase ZnO nanoparticles of similar size.

This observation is further supported by the EDS analysis in Fig. 5, which shows that the surface composition for ZnO is approximately: 35 at.% O and 65 at.% Zn, corresponding to mass percentages of 11.6% O

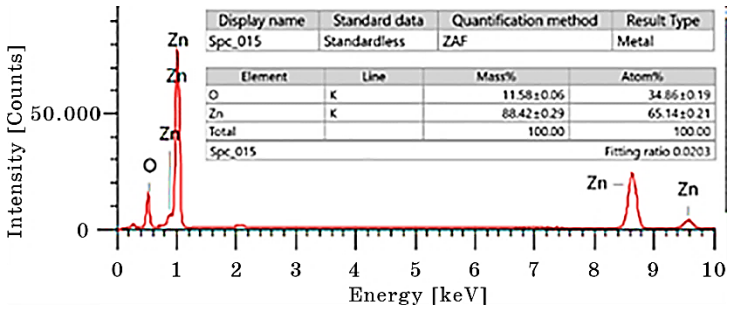


Fig. 5. EDS spectrum of the ZnO thin film grown on the Si substrate.

and 88.4% Zn.

The x-ray quantitative phase analysis of the Si/ZnO structure (Fig. 6*a*) revealed elemental contents of 74.6% Zn, 18.2% O, and 7.2% Si. As shown in Table 1, the average crystallite size, calculated using the Debye–Scherrer equation, was found to be approximately 28–35 nm. These results indicate that heating the substrate to 600°C prior to ZnO nanolayer deposition *via* magnetron sputtering is the most favourable condition. Under this regime, the substrate surface becomes well ordered, exhibits strong adhesion, and develops dense spherical structures, leading to complete coverage by a pure-phase ZnO thin film.

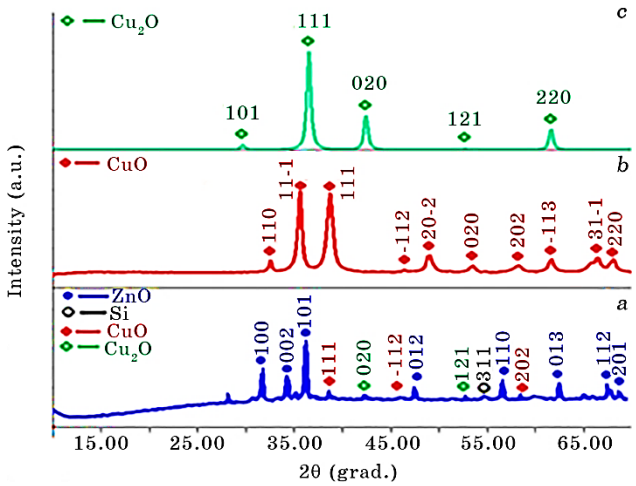


Fig. 6. XRD patterns of CuO and Cu_2O thin films grown on Si/ZnO substrates under different conditions: (*a*) without heating, (*b*) heated to 500°C, and (*c*) heated to 800°C with pre-cleaning by glow discharge ions.

TABLE 1. Quantitative phase and elemental composition of thin films grown on Si/ZnO under different conditions.

Sample/Condition	Elemental composition (%)	Phase composition (%)	Crystallite size (nm)
Si/ZnO (substrate)	Zn — 74.6, O — 18.2, Si – 7.2	ZnO — 100	28–35
Si/ZnO/CuO, no heating	Cu — 4.5, Zn — 56.9, O — 14.9, Si — 23.6	CuO — 1, Cu_2O — 4.6, ZnO — 70.9, Si — 23.6	≅14
Si/ZnO/CuO, 800°C	Cu — 79.9, O — 20.1	CuO — 100	≅14
Si/ZnO/ Cu_2O, 800°C	Cu — 88.8, O — 11.2	Cu_2O — 100	≅14

The main objective of this study was to deposit a thin copper oxide layer on the Si/ZnO surface prepared under the above conditions and to investigate its potential application in solar cells. To achieve this goal, the following experiments were conducted: CuO and Cu_2O thin films were grown on Si/ZnO samples under three different conditions, as shown in Fig. 6: *a*—without heating, *b*—heated to 500°C, and *c*—heated to 800°C. The x-ray phase analysis of the CuO and Cu_2O samples was used to determine their interplanar spacings, Miller indices, average crystallite sizes, quantitative and qualitative phase compositions, and degrees of crystallinity and amorphousness.

When CuO and Cu_2O thin layers were deposited on the Si/ZnO film surface without heating (Fig. 6*a*), the resulting layers were weakly bonded to the substrate, and numerous ZnO peaks were still visible in the XRD pattern. For the CuO sample grown at 800°C (Fig. 6*b*), the diffraction peaks were observed at $2\theta \cong 32.5°$, 35.5°, 38.7°, 48.8°, 53.4°, 58.2°, and 61.6°, corresponding to interplanar spacings $d_{hkl} \cong 2.75$ Å, 2.52 Å, 2.32 Å, 1.86 Å, 1.71 Å, 1.58 Å, and 1.50 Å, respectively. For Cu_2O (Fig. 6*c*), the diffraction peaks were found at $2\theta \cong 29.6°$, 36.2°, 42.4°, 52.6°, 61.5°, and 69.8°, with d_{hkl} values of approximately 3.01 Å, 2.46 Å, 2.13 Å, 1.74 Å, 1.50 Å, and 1.35 Å, respectively. In addition to peak identification, the amorphous–crystalline phases, quantitative phase composition, and qualitative phase analysis of CuO and Cu_2O are presented in Fig. 7.

Figure 7 shows the quantitative and qualitative phase analyses for: *a*—the Si/ZnO substrate, *b*—CuO and Cu_2O films deposited on Si/ZnO without heating, *c*—CuO films grown at 800°C, and *d*—Cu_2O films grown at 800°C. When CuO and Cu_2O were deposited without substrate heating (Fig. 7*b*), the quantitative analysis revealed elemental compositions of 4.5% Cu, 23.6% Si, 56.9% Zn, and 14.9% O. The qualitative phase analysis showed 1% CuO, 4.55% Cu_2O, 70.9% ZnO, and 23.6% Si. In contrast, when the substrate was heated to 800°C, the CuO sample (Fig. 7*c*) had a quantitative composition of 79.9% Cu and 20.1% O, with 100% CuO phase purity. Similarly, the Cu_2O sample (Fig. 7*d*) had a quantitative composition of 88.8% Cu and 11% O, with 100% Cu_2O phase purity (Table 1).

For the CuO thin films grown on Si/ZnO, the crystallite size was found to be approximately 14 nm, indicating the formation of nanostructured layers. When the samples were heated to 500°C and 600°C, the surface roughness gradually decreased, resulting in a smoother morphology. At 600°C, a uniformly ordered thin film composed of homogeneously distributed nanoparticles was successfully obtained.

Analysis of the spectrum in Fig. 9 obtained using the Raman spectroscopy method reveals three peaks corresponding to CuO at vibrational frequencies of 301, 363, and 623 cm^{-1}. In addition, peaks char-

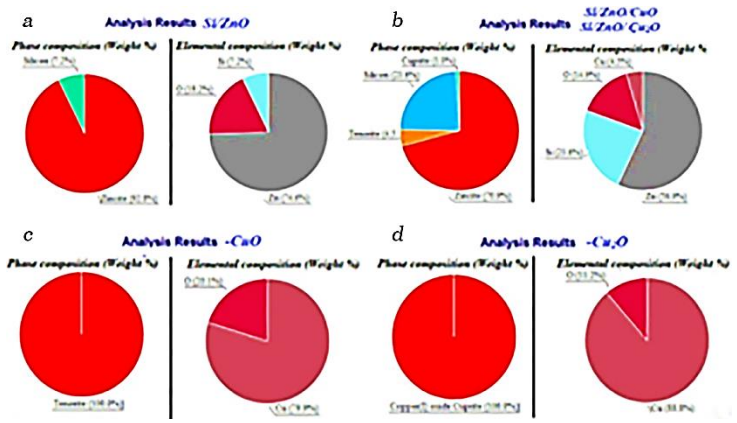


Fig. 7. Quantitative phase composition analysis of (*a*) Si/ZnO, (*b*) Si/ZnO/CuO and Si/ZnO/Cu_2O, (*c*) CuO, and (*d*) Cu_2O.

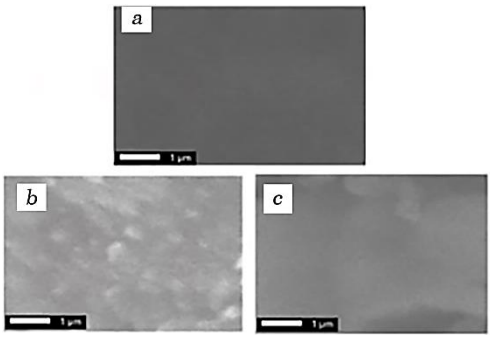


Fig. 8. SEM micrographs of: (*a*) CuO grown without substrate heating, (*b*) CuO grown at 500°C, and (*c*) Cu_2O grown at 800°C after glow-discharge ion cleaning of the substrate.

acteristic of Cu_2O at vibrational frequencies of 114, 141, 165, and 218 cm^{-1} are observed, which are associated with changes in microstructure or phase transitions induced by heating. The maximum positions of these peaks correspond to reported values for CuO [16], confirming that the chemical composition of the investigated element matches CuO. The peaks appearing after heating copper oxide to 800°C may be related to modifications in the crystal structure of CuO and Cu_2O, and indicate the coexistence of crystalline and amorphous-crystalline phases, as also shown in Fig. 10 and Table 2.

When the grown thin films of CuO and Cu_2O were examined separately using a Rigaku Oxford diffraction system (XtaLAB Synergy-i), the crystallographic structures and lattice parameters were determined as follows: for CuO, monoclinic $C12/c1$ with $a = 4.6832$ Å,

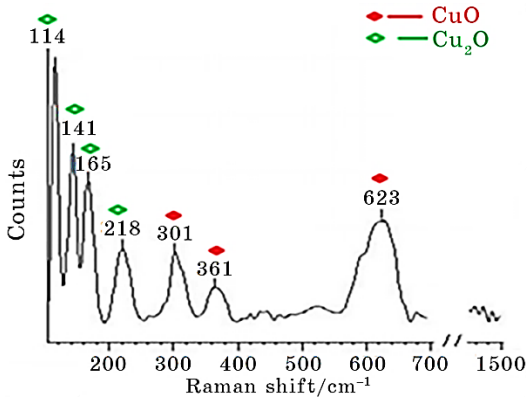


Fig. 9. Raman spectrum of copper oxide grown on the Si/ZnO surface *via* magnetron sputtering.

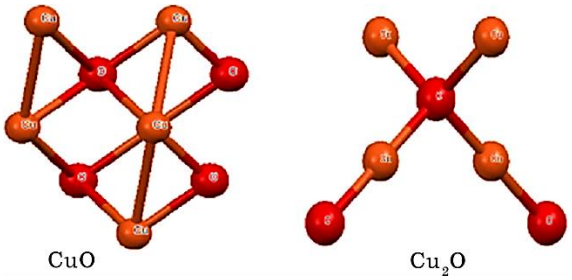


Fig. 10. X-ray structural analysis of CuO and Cu_2O thin films grown on the Si/ZnO surface.

TABLE 2. Crystallographic parameters of CuO and Cu_2O thin films grown on Si/ZnO.

Material	Crystal system	Space group	Lattice parameters (Å)	Main diffraction peaks (2θ, °)	Raman active modes (cm^{-1})
CuO	Monoclinic	$C12/c1$	$a = 4.6832$, $b = 3.4288$, $c = 5.1297$	32.5, 35.5, 38.7, 48.8, 53.4, 58.2, 61.6	301, 363, 623
Cu_2O	Cubic	$Pn{-}3m$	$a = 4.2580$	29.6, 36.2, 42.4, 52.6, 61.5, 69.8	114, 141, 165, 218

$b = 3.4288$ Å, and $c = 5.1297$ Å; for Cu_2O, cubic $Pn{-}3m$ with $a = 4.2580$ Å.

4. CONCLUSION

In this study, CuO and Cu_2O thin-film heterostructures were fabricated on Si/ZnO substrates using the magnetron sputtering method. Experiments were carried out under three different conditions: without heating, with substrate heating at 600°C, and with heating at 600–800°C followed by surface cleaning using glow discharge ions. The crystallinity, phase composition, morphology, as well as the electrophysical and optical properties of the obtained layers were thoroughly investigated. The analyses revealed that substrate preheating at high temperatures combined with ion cleaning significantly enhanced crystallinity, resulting in smooth, dense structures with a pure phase composition. In particular, for Cu_2O layers grown on ion-cleaned surfaces at 800°C, a 100% crystalline phase was achieved. SEM and EDS analyses, along with Raman spectroscopy, confirmed these findings. The results demonstrate that appropriate temperature control and surface pretreatment can substantially improve the quality of copper oxide semiconductor layers. Consequently, the fabricated CuO/Cu_2O heterostructures can be proposed as promising materials for the development of efficient and environmentally friendly solar cells.

AUTHORS' CONTRIBUTIONS

I. O. Kosimov conceived the research idea and led the research. carried out the electronic structure using theoretical calculations. Sh. T. Khozhiev developed the project, reviewed the literature and collected data on electronic and mechanical properties, supervised the results of this work and wrote the manuscript taking into account the contributions of all authors. K. T. Dovranov supervised the project, developed the main conceptual ideas, checked the analytical approaches and provided critical feedback. M. A. Davlatov conducted thin-film deposition experiments and contributed to the analysis of electrophysical properties. F. F. Arzikulov participated in the experimental design and preparation of samples. U. Kh. Kholikov performed experimental work and thin film deposition and performed structural, optical analysis. All authors approved the final version of the manuscript.

REFERENCES

1. T. Minami, Y. Nishi, T. Miyata, and J. I. Nomoto, *Appl. Phys. Express*, **4**, No. 6: 062301 (2011).
2. A. Mittiga, E. Salza, F. Sarto, M. Tucci, and R. Vasanthi, *Appl. Phys. Lett.*, **88**, No. 16: 163502 (2006).
3. M. Izaki, T. Shinagawa, K. T. Mizuno, Y. Ida, M. Inaba, and A. Tasaka, *J. Phys. D: Appl. Phys.*, **40**, No. 11: 3326 (2007).

4. S. S. Jeong, A. Mittiga, E. Salza, A. Masci, and S. Passerini, *Electrochim. Acta*, **53**, No. 5: 2226 (2008).
5. M. Izaki, K. T. Mizuno, T. Shinagawa, M. Inaba, and A. Tasaka, *J. Electrochem. Soc.*, **153**, No. 9: C668 (2006).
6. K. Fujimoto, T. Oku, T. Akiyama, and A. Suzuki, *J. Phys.: Conf. Ser.*, **433**: 012024 (2013).
7. K. Nakaoka and K. Ogura, *J. Electrochem. Soc.*, **149**, No. 11: C579 (2002).
8. K. Fujimoto, T. Oku, and T. Akiyama, *J. Ceram. Soc. Jpn.*, **119**, No. 1390: 402 (2011).
9. T. Oku, T. Noma, A. Suzuki, K. Kikuchi, and S. Kikuchi, *J. Phys. Chem. Solids*, **71**, No. 4: 551 (2010).
10. T. Oku, R. Motoyoshi, K. Fujimoto, T. Akiyama, B. Jeyadevan, and J. Cuya, *J. Phys. Chem. Solids*, **72**, No. 11: 1206 (2011).
11. M. I. Domnina, S. K. Filatov, I. Zyuzyukina, and L. P. Vergasova, *Neorg. Mater.*, **22**: 1743 (1986).
12. M. A. Davlatov, K. T. Davranov, X. T. Dovranov, S. N. Xusanov, A. R. Kodirov, and S. Xolikulova, *East Eur. J. Phys.*, **2**: 330 (2025).
13. H. Kidowaki, T. Oku, and T. Akiyama, *J. Phys.: Conf. Ser.*, **352**: 012022 (2012).
14. T. Oku, A. Takeda, A. Nagata, K. Fujimoto, T. Akiyama, and A. Suzuki, *J. Phys.: Conf. Ser.*, **352**: 012024 (2012).
15. K. T. Dovranov, M. Vinnichenko, M. Normuradov, X. Davranov, D. Nabiyev, M. Davlatov, A. Kodirov, P. Parmonov, and N. Kurbonov, *Proc. Int. Conf. Electrical Engineering and Photonics (EExPolytech)* (2024), p. 308.
16. T. Oku, A. Takeda, A. Nagata, R. Motoyoshi, K. Fujimoto, T. Noma, and E. Ōsawa, *Light Harvesting Nanomaterials* (Bentham Science Publishers: 2015).
17. K. T. Dovranov, M. T. Normuradov, M. A. Davlatov, K. T. Dovranov, T. Toshev, and N. Kurbonov, *East Eur. J. Phys.*, No. 3: 350 (2024).
18. P. Engelhart, N. P. Harder, R. Grischke, A. Merkle, R. Meyer, and R. Brendel, *Prog. Photovolt. Res. Appl.*, **15**, No. 3: 237 (2007).
19. B. K. Meyer, A. Polity, D. Reppin, M. Becker, P. Hering, P. J. Klar, and C. Ronning, *Phys. Status Solidi B*, **249**, No. 8: 1487 (2012).